AIAA 80-1035R

Propeller Signatures and Their Use

J. F. Johnston,* R. E. Donham,† and W. A. Guinn‡
Lockheed-California Company, Burbank, Calif.

The identification and use of the noise and vibration signatures of individual propellers, described herein, has provided a basis for rational advances in propeller-noise analysis and control. These signatures, or influence vectors, were used for 1) analytically determining optimum synchrophase angles and 2) diagnosing the specific paths—airborne and structure-borne—of the noise into the cabin. A number of significant conclusions are drawn from flight experiments in a Navy P-3C patrol aircraft. The results and techniques from this work are applicable to improving the passenger and crew comfort as well as equipment life in propeller-powered aircraft.

Introduction

THE identification of the noise and vibration signatures of individual propellers has provided a basis for rational advances in propeller noise/vibration analysis and control. This paper describes the derivation of the signatures and gives some examples of their use. The work is based on tests performed by Hamilton Standard and the Naval Air Test Center (NATC) on a Navy/Lockheed P-3C four-engine patrol aircraft in 1978. The data analysis and the development of the signature identification computer code LOCKPHASE were performed at Lockheed in 1979.

Aircraft and Tests

The test airplane was a standard Navy/Lockheed P-3C based at Naval Air Test Center (NATC), Patuxent River, Md. This was a joint NATC/Hamilton Standard test program in which Hamilton Standard provided the instrumentation and NATC performed the tests under the sponsorship of Naval Air Systems Command (NAVAIR). Hamilton Standard made the test tapes available to Lockheed in early 1979.

Instrumentation

Noise and vibration were recorded at the twelve locations shown in Fig. 1 by use of a fourteen-channel tape recorder with a multiplex system that allowed recording of four data signals per channel. Recordings were made in the frequency modulation (FM) mode which allowed flat frequency response from 0 to 1000 Hz. In addition to noise and vibration, a once-per-revolution signal (the propeller "pip") from each of the propellers was recorded to allow evaluation of the relative phase of the four propellers.

Bruel and Kjaer half-inch condenser microphones (Type 4133) mounted at seated ear height were used at all noise measurement locations. They were calibrated before flight. These were mounted at locations in free space to minimize the increase in noise due to pressure doubling effects that can occur when a microphone is mounted on a solid surface. The vibration pickups, Vibramite Types 11, 14, or 14C were mounted on the floor of the aircraft at locations below the microphones on seat rails or other rigid structure to avoid amplification of the vibration signal that can occur when measurements are made on an unsupported panel.

Presented as Paper 80-1035 at the AIAA 6th Aeroacoustics Conference, Hartford, Conn., June 4-6, 1980; submitted July 21, 1980; revision received May 18, 1981.

*Senior Research and Development Engineer.
†Research and Development Engineer. Member AIAA.
‡Senior Research Scientist. Member AIAA.

Tests

Two test series were conducted. The first series was with the propeller balance "as is," and the second with the propellers dynamically balanced. They were about three weeks apart. The specific tests conducted are given in Table 1. Runs A-D were in the first series, and runs E-H in the second series.

The propeller signatures were determined from run A, the mechanical governing run. They have been used to "predict" the results of runs B, E, and G. Note: run G had the two outboard propellers feathered, with increased horsepower to the two inboards.

Propeller Signatures

Theory

Each propeller in a multipropeller aircraft contributes differently to the noise and vibration in the aircraft. The individual propeller contribution at any location is called its signature at that location. It consists of complex waves having components at frequencies equal to the blade passage frequency NP (N=number of blades, P=per revolution), and integer multiples of the blade passage frequency kNP, where k is an integer. In this discussion the magnitude and phase of a given frequency component of the contribution will be called its signature at that frequency.

This signature can be determined from test data. In a two-propeller airplane it can be determined directly by feathering one propeller and measuring the amplitude and phase of the noise or vibration due to the other propeller. In the four-propeller airplane it is not usually practical to feather three of the four propellers, so indirect means must be used. Those means are discussed in this section.

Figure 2 is an illustration of signature vectors for noise at a specific location in a four-engine airplane. The sound pressure vectors S_1, S_2, S_3, and S_4 arrive from similarly numbered propellers. The length of each vector represents the pressure amplitude at that location due to that propeller. The phase ϕ_1, ϕ_2, etc., is the fraction of the wavelength by which the vector leads the propeller "pip" which marks the propeller passing the reference position. Inasmuch as the kNP wave pattern repeats itself kN times per revolution, the vector rotates kN deg for every degree of propeller rotation ψ (Fig. 3). For a four-bladed propeller the $4P$ vector rotates 4 deg per degree of propeller rotation, the $8P$ vector rotates 8 deg per 1 deg, etc. In Figs. 2 and 3 the propeller reference position is blades-level. The actual position may be arbitrary, as long as it is the same for all propellers.

Also for convenience, the No. 1 propeller is used here as the phase reference; note that is shown at the reference position in Fig. 3 and will be assumed at the reference position in the remaining discussion.

The signatures or influence vectors add as shown in Fig. 3, which represents the $4P$ components. For the propeller phase angles on the left, the vectors nearly close, giving a low net

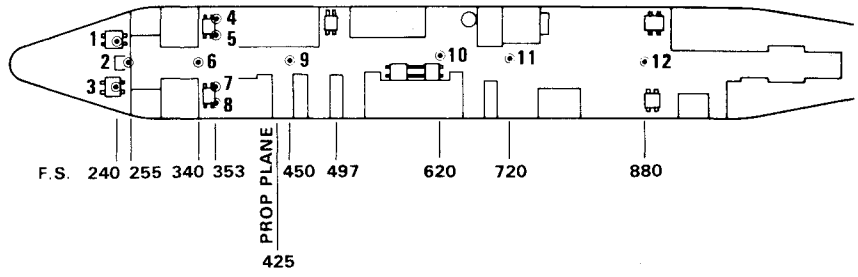

Fig. 1 P-3 aircraft measurement locations.

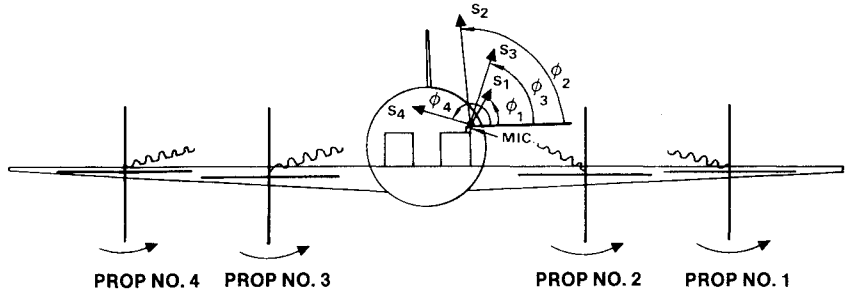

Fig. 2 Propeller signatures.

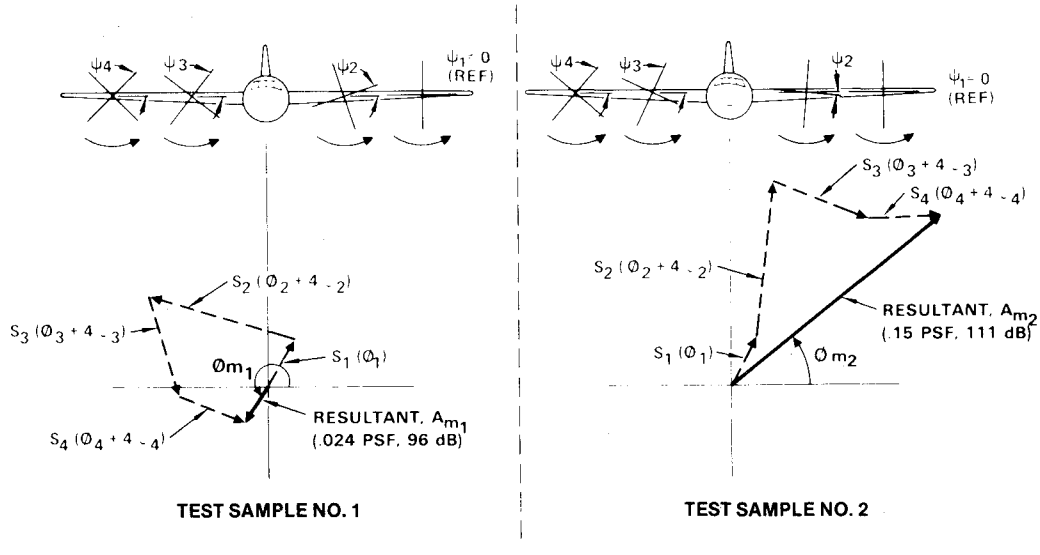

Fig. 3 How signatures add.

Table 1 Engine and propeller operating conditions for P-3 noise and vibration test[a]

Test phase	Run	Mode of operation	Propeller percent rpm/engine horsepower			
			Propeller No. 1	Propeller No. 2	Propeller No. 3	Propeller No. 4
I	A	Mechanical governing	100.5%/2150	99.2%/2150	100.0%/2150	99.6%/2150
I	B	Synchrophasing	100.5%/2125	99.8%/2125	99.8%/2150	100.6%/2100
I	C		100.5%/100	99.7%/2950	99.5%/2950	100.6%/200
I	D		100.5%/2840	99.6%/150	100.6%/210	100.6%/3000
III	E	Mechanical governing	100.4%/2200	99.3%/2200	100.0%/2200	99.9%/2200
III	F	Synchrophasing	100.5%/2200	99.8%/2160	99.8%/2200	100.6%/2200
III	G		0/0	99.8%/2920	99.4%/2920	0/0
III	H		100.6%/2900	99.7%/1200	99.6%/1200	100.7%/2985

[a] All tests were conducted at 20,000-ft altitude at 233 knots indicated air speed. For runs B and F No. 3 was the master propeller. Specified settings were propeller No. 1 at 41-deg lag, propeller No. 2 at 14-deg lag, and propeller No. 4 at 11-deg lag.

pressure amplitude of 0.024 psf, or 96 dB. A 20-deg retardation of the No. 2 propeller (an 80-deg retardation of its signature vector) and a 15-deg advance of the No. 3 propeller (60-deg advance of its vector) as shown on the right, result in a much larger net vector, 0.15 psf, 111 dB. It is apparent from this example that when the signatures are known, the effect of the relative propeller phasing can be calculated easily.

To determine the signatures from test data, it is theoretically necessary only to measure the sound pressure (or vibration) vector at four different known combinations of propeller phases. In practice the accuracy is improved by using more data points in a least-squares determination, which is included in the computer code LOCKPHASE, a FORTRAN program developed for signature analysis.

The basic equation assumes local linearity, i.e., that the contribution of each propeller is vectorially additive in arriving at the net noise or vibration at a given position. In complex notation, and using the No. 1 propeller as the reference for phase, the $4P$ noise (as an example) is divided into "real" (cosine) and "imaginary" (sine) components.

$$A_{\mathrm{Re}} = A_m \cos\phi_m = S_1 \cos(\phi_1) + S_2 \cos(\phi_2 + 4\psi_2) + S_3 \cos(\phi_3 + 4\psi_3) + S_4 \cos(\phi_4 + 4\psi_4)$$

$$A_{\mathrm{Im}} = A_m \sin\phi_m = S_1 \sin(\phi_1) + S_2 \sin(\phi_2 + 4\psi_2) + S_3 \sin(\phi_3 + 4\psi_3) + S_4 \sin(\phi_4 + 4\psi_4)$$

See Figs. 2 and 3 for definition of terms. The A_m, ϕ_m, and ψ_2, ψ_3, ψ_4 are measured test data; the signatures S_n, ϕ_n are to be determined. The 4ψ terms are replaced by 8ψ or 12ψ when dealing with $8P$ or $12P$ signatures, respectively.

In matrix notation, the equations become

$$[A] = [\psi][S]$$

The least-squares form for use with more than the minimum data sets is obtained by premultiplying both sides by $[\psi]^T$, the transpose of the (nonsquare) ψ matrix. Solution for the signatures then follows by premultiplying both sides by $[[\psi]^T[\psi]]^{-1}$, the inverse of the resulting square matrix of ψ. This gives

$$[S] = [[\psi]^T[\psi]]^{-1}[\psi]^T[A]$$

where

$$[\psi] = \begin{bmatrix} a & \begin{matrix} 1 & 0 & \cos4\psi_2 - \sin4\psi_2 \ldots \cos4\psi_4 - \sin4\psi_4 \\ 0 & 1 & \sin4\psi_2 \cos4\psi_2 \ldots \sin4\psi_4 \cos4\psi_4 \end{matrix} \\ b & \begin{matrix} 1 & 0 & \cos4\psi_2 - \sin4\psi_2 \ldots \cos4\psi_4 - \sin4\psi_4 \\ 0 & 1 & \sin4\psi_2 \cos4\psi_2 \ldots \sin4\psi_4 \cos4\psi_4 \end{matrix} \\ & \vdots \\ n & \begin{matrix} 1 & 0 & \cos4\psi_2 - \sin4\psi_2 \ldots \cos4\psi_4 - \sin4\psi_4 \\ 0 & 1 & \sin4\psi_2 \cos4\psi_2 \ldots \sin4\psi_4 \cos4\psi_4 \end{matrix} \end{bmatrix}$$

(The $a, b, \ldots, n$ sets of data are indicated.)

$$[A] = \begin{bmatrix} & \text{Mic 1} & \text{Mic 2} & \text{Mic 12} \\ a & \begin{matrix} A_{1_a}\cos\phi_{1_a} & A_{2_a}\cos\phi_{2_a} \ldots A_{12_a}\cos\phi_{12_a} \\ A_{1_a}\sin\phi_{1_a} & A_{2_a}\sin\phi_{2_a} \ldots A_{12_a}\sin\phi_{12_a} \end{matrix} \\ & \vdots \\ n & \begin{matrix} A_{1_n}\cos\phi_{1_n} & A_{2_n}\cos\phi_{2_n} \ldots A_{12_n}\cos\phi_{12_n} \\ A_{1_n}\sin\phi_{1_n} & A_{2_n}\sin\phi_{2_n} \ldots A_{12_n}\sin\phi_{12_n} \end{matrix} \end{bmatrix}$$

(Note that 12 data sensors are assumed in the above example.)

$$[S] = \begin{array}{c} \begin{matrix} \text{Mic 1} & \text{Mic 2} & \text{Mic 12} \end{matrix} \\ \begin{bmatrix} S_{11_R} & S_{21_R} \ldots\ldots & S_{12-1_R} \\ S_{11_I} & \cdot & S_{12-1_I} \\ S_{12_R} & \cdot & \cdot \\ S_{12_I} & \cdot & \cdot \\ S_{13_R} & \cdot & \cdot \\ S_{13_I} & \cdot & \cdot \\ S_{14_R} & \cdot & S_{12-4_R} \\ S_{14_I} & S_{24_I} \ldots\ldots & S_{12-4_I} \end{bmatrix} \end{array}$$

The numerical subscripts of the $[A]$ terms refer to the sensor number, and the subscripts of the $[\psi]$ terms refer to the propeller number. In the $[S]$ terms, the first numerical subscript refers to the sensor number, and the second to the propeller number.

Signature Determination from Test Tapes

Data for the signature determinations are obtained by analyzing the propeller position pips for propeller relative phase, ψ, and the microphone and vibration pickups for $4P$, $8P$, etc., amplitude and phase.

The position pips, Fig. 4, were not of a form that could be analyzed by frequency response techniques. Therefore, time-domain cross correlation techniques were used, in which the time shift required to superimpose reference and test pips was determined. This correlation was performed on a Time/Data 1923/90 time series data analysis system. The correlation was determined to 0.0001 s, or 0.6-deg relative phase at 17 rps. A sample repetition, performed months after the first determination, repeated the 30 original phase data points "exactly" to this degree of definition.

The pressure or vibration data were analyzed by the hard-wired Fast Fourier Transform (FFT) capability of the same 1923/90 system. Special consideration here was that the data sample should be as short as possible (because the responses were changing rapidly as the relative propeller phases varied), but the period must be an integer submultiple of the 68-Hz blade passage frequency and its harmonics. The requirements were satisfied by selecting a 0.25-s sample time. Inasmuch as the frequency interval is the reciprocal of the sample time, this selection gave a 4-Hz frequency interval; i.e., the frequency response was defined at 64, 68, and 72 Hz, at 132, 136, and 140 Hz, at 200, 204, and 208 Hz, etc., where the center frequency in each group is the one of interest. The definition becomes poor at the higher harmonics if the blade passage frequency is not exactly 68 Hz. For example, the 208-Hz amplitudes were nearly as great as the 204-Hz amplitudes, indicating that the peak was above 204 Hz.

This inaccuracy is reduced by determining the signatures from steady-state tests in which data are taken at a number of different constant propeller phase angle settings. In this case larger sample times, such as 1.0 s, can be used, giving a frequency definition to the nearest 1.0 Hz.

The propeller pips should be read over about the same interval as the data sample. For the mechanical governing case, they were sampled over a 0.1-s interval starting coincident with the start of the 0.25-s data sample. Where the data sample is 1.0 s, the pips will be averaged over 8 consecutive 0.1-s samples starting coincident with the data samples. In all cases the start of data sample is exactly when propeller No. 1

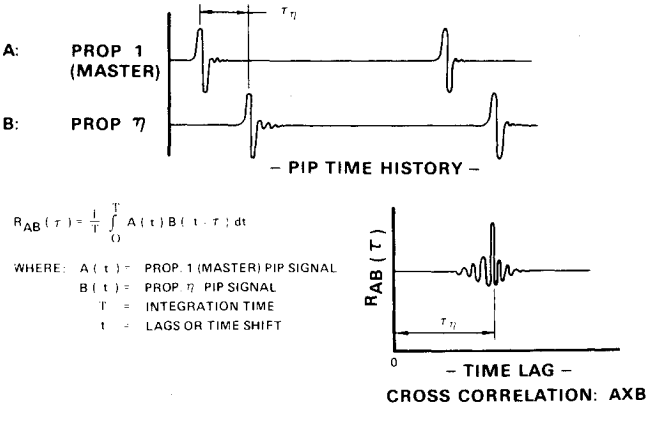

- THE CROSS CORRELATION FUNCTION OF A WAVEFORM, A(t) WITH B(t) PROVIDES A MEASURE OF THE SIMILARITY BETWEEN ITSELF, A(t), AND A TIME-SHIFTED WAVE FORM, B(t).
- THE WAVEFORMS ARE SAID TO CORRELATE FOR VALUES OF τ THAT PRODUCE LARGE POSITIVE VALUES OF $R_{AB}(\tau)$

Fig. 4 Cross correlation function.

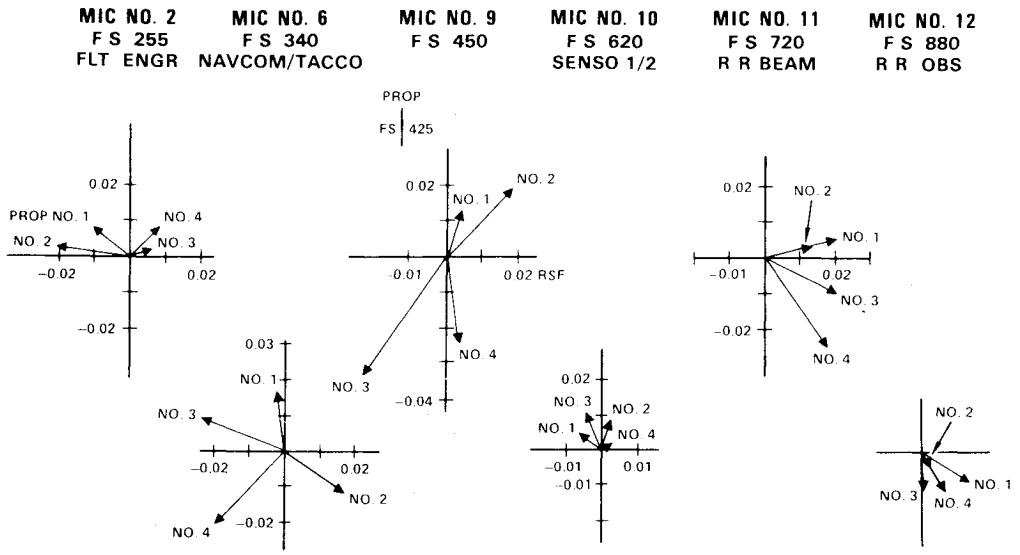

Fig. 5 Signatures along centerline: 68-Hz noise, P-3C aircraft.

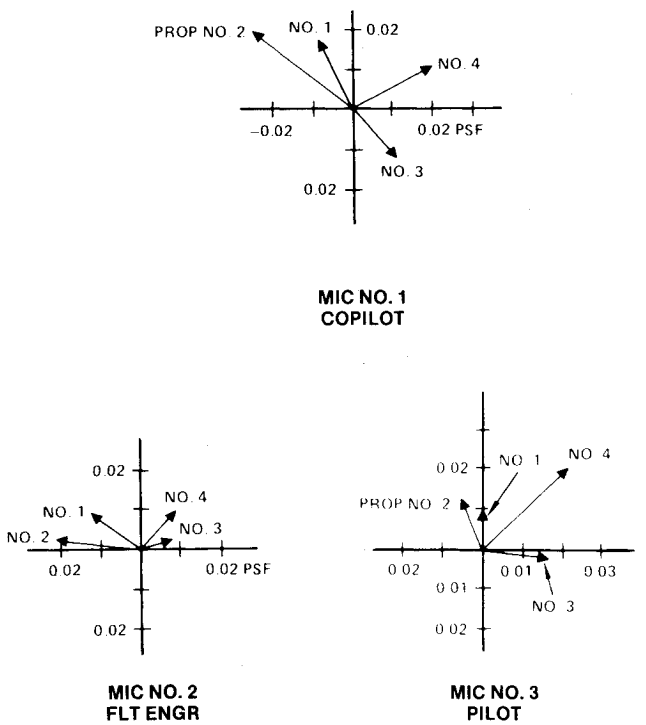

Fig. 6 Signatures at flight stations: 10-point avgs, 68-Hz noise, P-3C aircraft.

passes the reference position. The sample times and number of samples on the 1923/90 can be selected in integer exponents of 2.

Signature Vector Plots

The 68-Hz sound pressure signatures of the P-3C determined from ten test data times taken arbitrarily at 10-s intervals in run A, the mechanical governing run, are given in Figs. 5-7. Figure 5, showing the signatures along the cabin centerline from front to rear, shows major activity is in the vicinity of the propeller plane, with a secondary peak over the wing rear beam. The outboard propeller contributions are surprisingly large, even in the forward cabin. They predominate over the wing rear beam and aft. The cross section at the flight station, Fig. 6, shows higher activity at the sides than at center, again with surprisingly large contributions from the outboard propellers. The cross section at the tactical coordinator (TACCO) and navigator/communicator (NAVCOM) stations, Fig. 7, shows very high activity on the left side, microphone No. 8. The adjacent propeller, No. 2, is the largest contributor, as would be expected since the blades of that propeller are more highly loaded than average as they pass next to the fuselage. The large size of the contributions from the other propellers at microphone No. 8 indicates that the left side in this section is a hot spot producing excessive noise transmission. Simple modifications here might result in large noise reductions.

The magnitudes of the noise contributions in decibels can be judged from the following equivalents:

0.084 psf	= 106 dB
0.042 psf	= 100 dB
0.021 psf	= 94 dB
0.0105 psf	= 88 dB
0.0052 psf	= 82 dB

Vibration Signatures

The 68-Hz floor vibration signatures, taken at the same times as the noise signatures, are plotted in Figs. 8-10. The signatures along the center, Fig. 8, are similar to the noise, Fig. 5, in that they show highest activity near the propeller plane and a secondary peak over the wing rear beam, F.S. 720. The flight stations show very low vibration, Fig. 9. The forward crew stations at F.S. 350, Fig. 10, show that the vibration peaks on centerline and is lowest near the sides. This variation is opposite that of the noise, Figs. 6 and 7, which tend to peak at the sides.

In all cases high coherencies, on the order of 80-95%, were found between the vibrations and the adjacent noise. Since the coherency is a measure of the degree to which the signals are linearly related, this reinforces the strong noise/vibration relations expected theoretically.

At 68 Hz, the normal acceleration levels in g's are about 10% above the plotted vibration levels in inches per second. On this basis the largest signature, that of propeller No. 3 at Vib No. 9, Fig. 8, is ± 0.2 g.

Validation

The first validation of the calculated signatures was by using the signatures to calculate back (reconstruct) the magnitude and phase of the test data points from which the signatures were determined. The second and more meaningful validation was to predict the results of other tests. In this case the signatures determined from run A, the mechanical

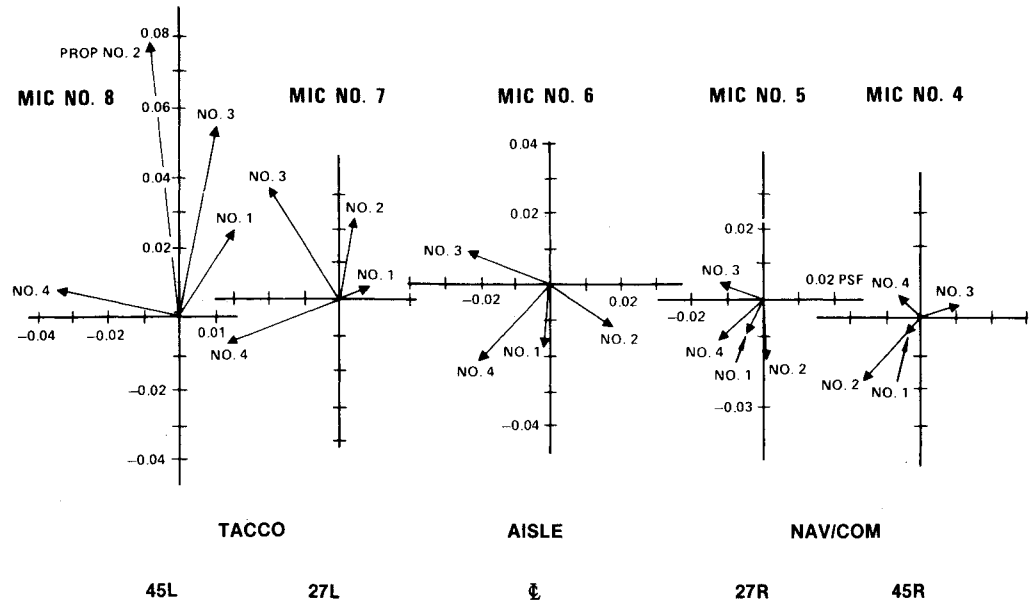

Fig. 7 Signatures at forward crew station: 68-Hz noise.

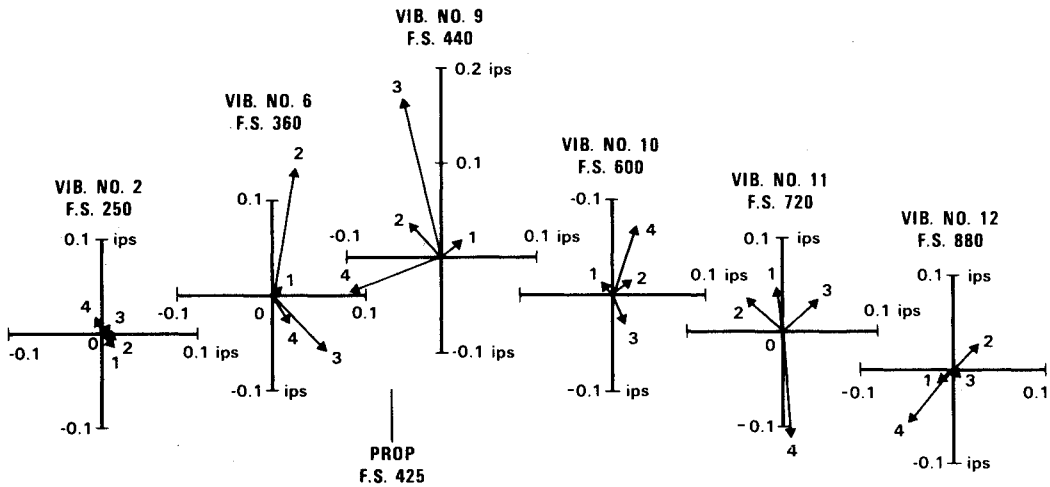

Fig. 8 68-Hz vibration signatures along centerline.

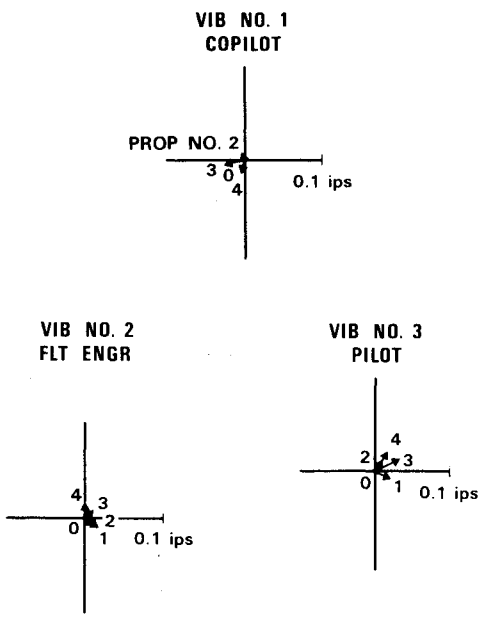

Fig. 9 68-Hz vibration signatures at flight stations.

governing run, were used to "predict" the results of run B, the synchrophase run, in the same flight, and runs E and G (see Table 1) in a second flight made about three weeks later. In each case the input data were the signatures fron run A and the measured propeller phase angles from the later runs.

Reconstruction

A typical test data reconstruction from signatures is shown in Fig. 11 for microphone 8 in run A. The ten test vectors from which the four signatures were determined are labeled A-J. The reconstructions, A^1-J^1, show good agreement in amplitude and generally good agreement in phase. The larger vectors showed 4*P* phase errors less than 10 deg (2.5 deg of propeller rotation). This initial validation was considered good.

4P, 8P, and 12P Noise Correlations

The 4*P*, 8*P*, and 12*P* noise signatures calculated from ten points in run A, the mechanical governing run, were used to predict the amplitudes of ten points in run B, arbitrarily selected at 10-s intervals. The propeller phase changes in run B were about ±5 deg, Fig. 12. The 4*P* amplitude variations, Fig. 13, were reasonably predicted. The 8*P* predictions, Fig.

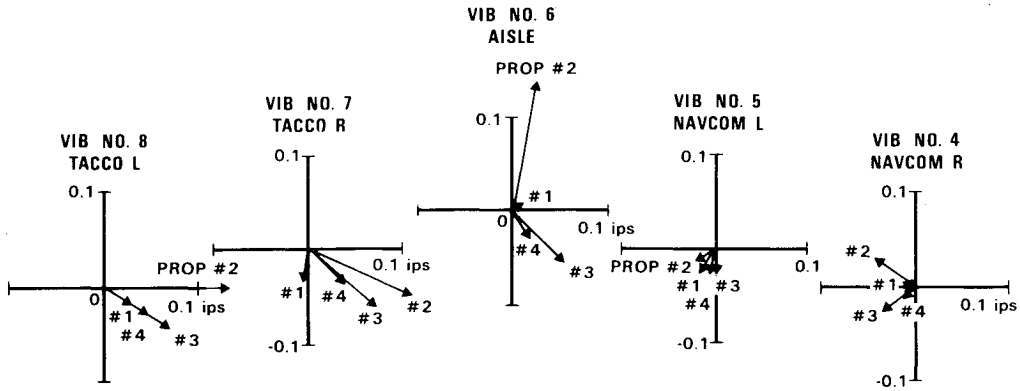

Fig. 10 68-Hz vibration signatures at F. S. 350.

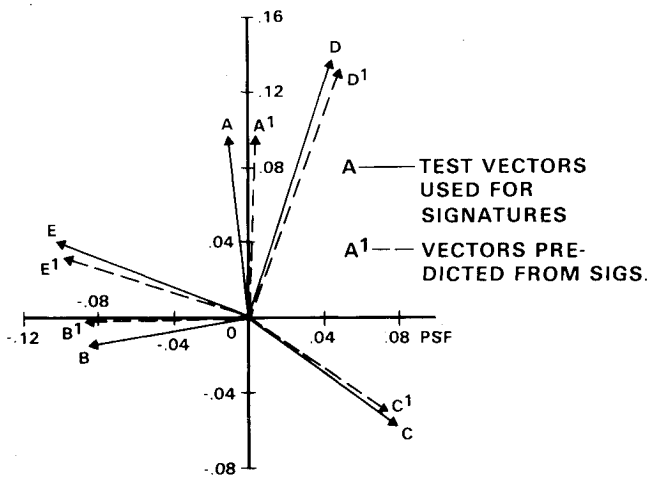

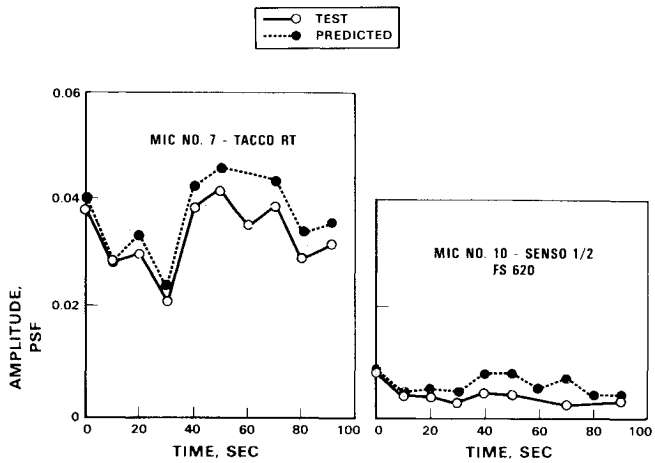

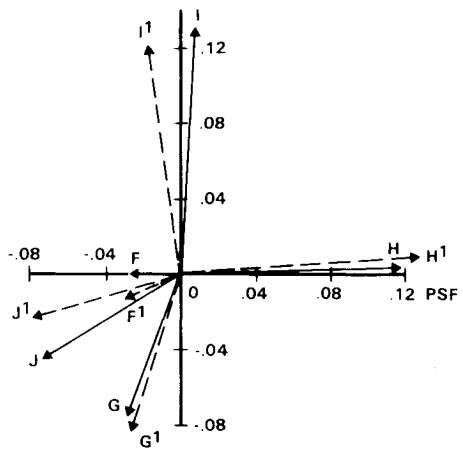

Fig. 11 Data reconstruction for 68-Hz noise.

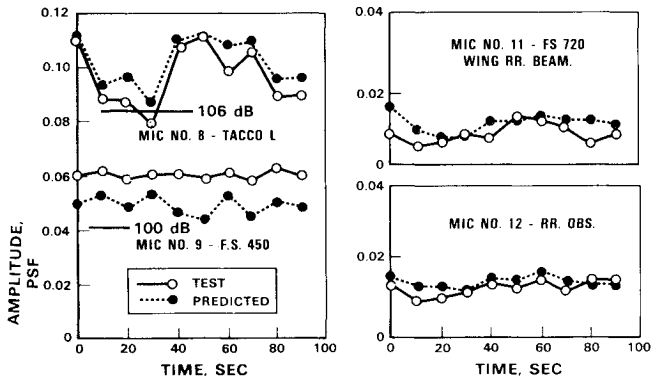

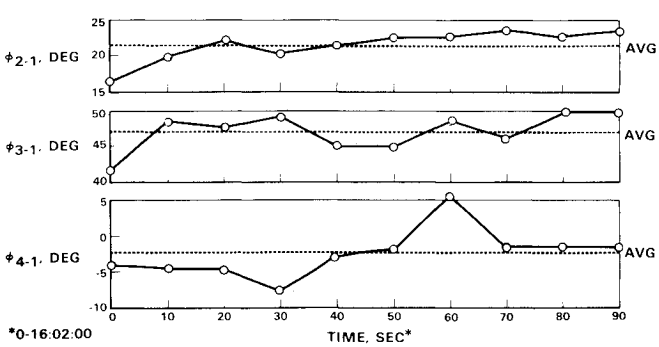

Fig. 12 Phase variation in synchrophase run.

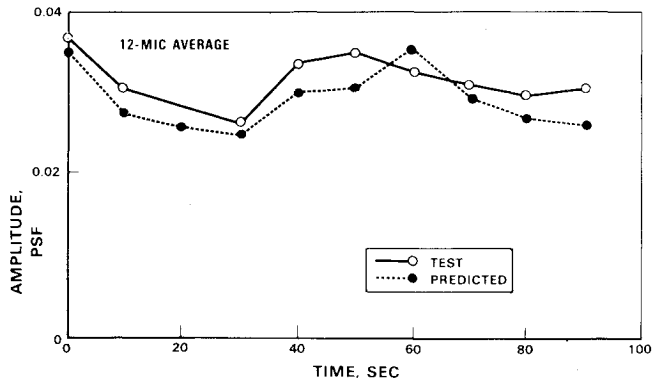

Fig. 13 4*P* noise during synchrophase run.

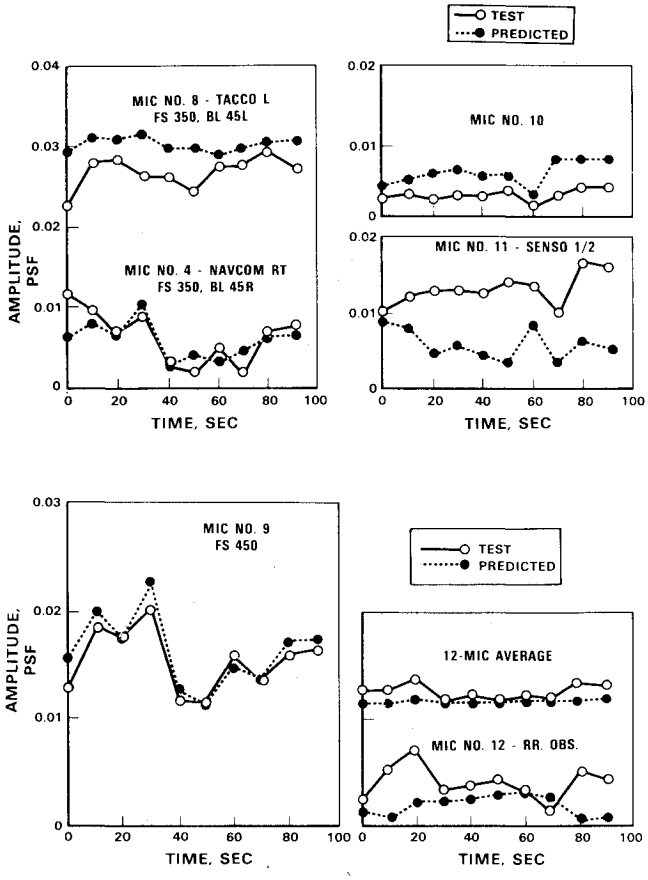

Fig. 14 8*P* noise during synchrophase run.

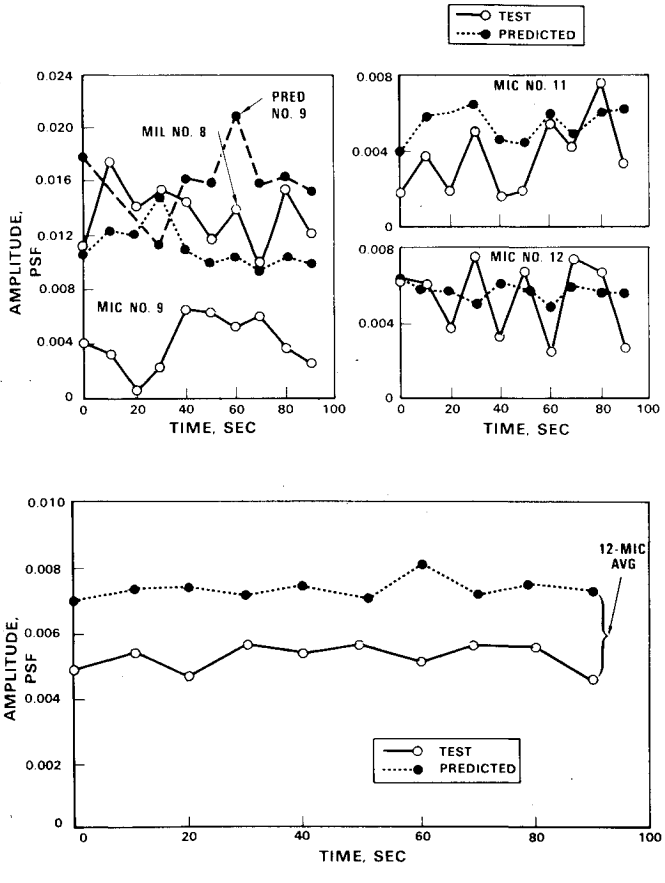

Fig. 15 12*P* noise during synchrophase run.

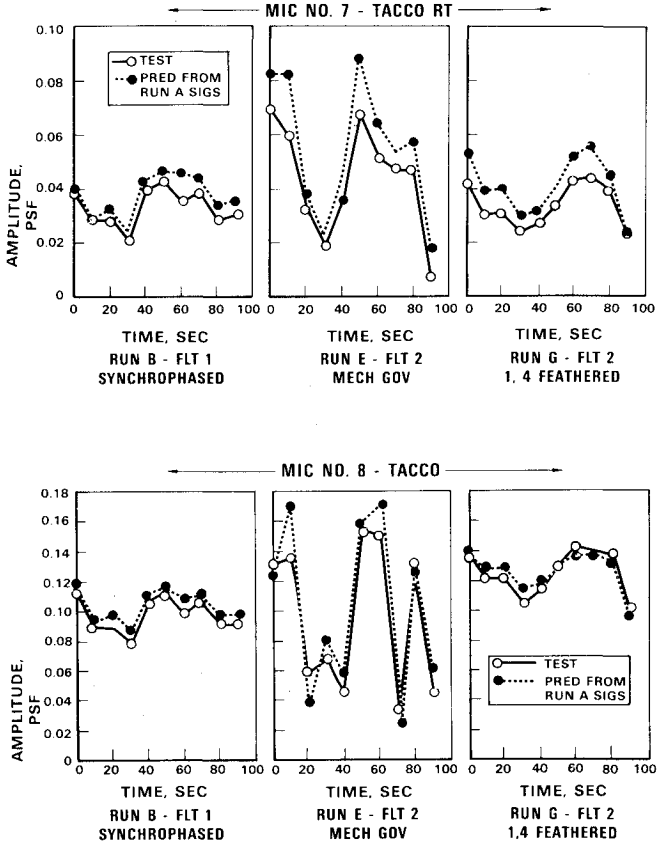

Fig. 16 68-Hz signature validation.

14, were not as good, although some showed excellent matches. The 12*P* predictions, Fig. 15, were still poorer.

It was concluded that the higher harmonics, 8*P* and up, were not verified, but the 4*P* data could be used with some caution. Future propeller signatures should be obtained from steady-state tests in which data are taken at various constant propeller phase angle combinations. The remainder of the P-3 noise data discussion is limited to the 4*P* content.

4P Noise Predictions for Runs E and G

Figure 16 presents typical 4*P* test/prediction comparisons in three runs: run B, already presented; run E, a mechanical governing run taken three weeks later; and run G, in which the outboard propellers were feathered and the inboard engines were increased in power—from about 2000 hp each for the other runs to about 3000 hp each for run G. Here the predictions were made to determine whether there was a consistent offset to indicate the effect of power on the magnitude of the signatures, inasmuch as the predictions were made for the 2000-hp condition.

The plots show that the large variations in run E were predicted very satisfactorily.

The outboard-feathered run was predicted well. It need hardly be remarked that such a two-propeller prediction from four-propeller data is unprecedented. Surprisingly, there was no average offset of test above predictions to show an effect of the 50% change in power.

Based on these validations, it was concluded that the P-3C 4*P* noise signatures were satisfactory for most engineering uses, although very detailed conclusions and diagnostics should not be attempted until better signatures, based on steady-state data, are obtained.

P-3C Vibration Correlations

Similar results were obtained for the vibration correlations. It was concluded that the P-3C 4*P* vibration signatures are verified and can be used for predictive and diagnostic analyses. The 8*P* vibration signatures may be used if required.

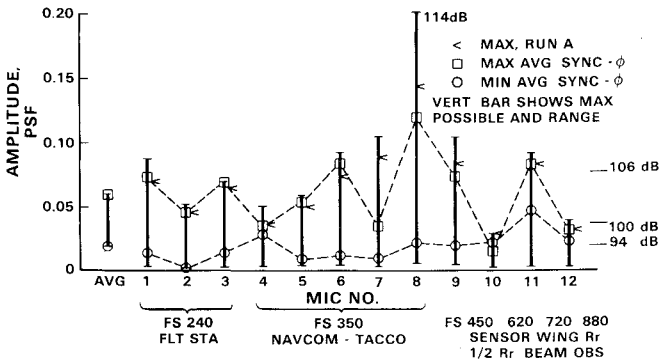

Fig. 17 Synchrophase effects on 68-Hz noise.

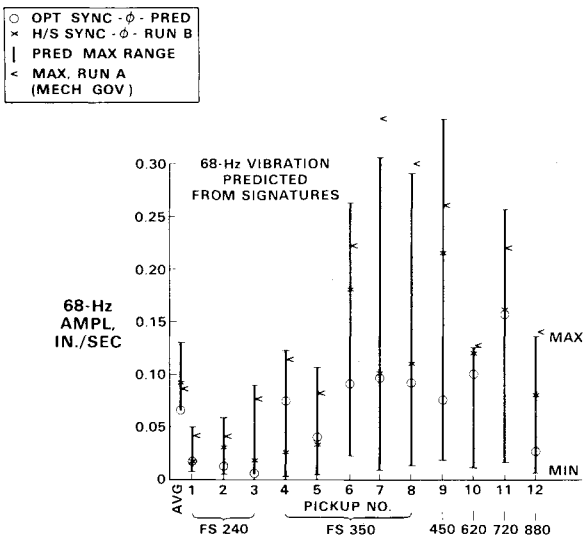

Fig. 18 Synchrophase effect on 68-Hz vibrations.

Use of Signatures

Propeller signatures permit a rational correlation of test results (hitherto embarrassingly impossible), a technique for determining analytically optimum synchrophase angles for each flight condition, and, most importantly for future progress, a means for understanding and diagnosing the noise/vibration sources and paths. Some of these uses are discussed in the following.

Optimum Synchrophase Selection by Analysis (LOCKPHASE) 68-Hz Noise

With the signatures, optimum synchrophase can be determined mathematically. The 5832 possible combinations of 5-deg steps were investigated for P-3C noise and vibration at twelve locations using the LOCKPHASE program, as shown in Figs. 17 and 18. The individual microphones, Fig. 17, varied from as high as 114 dB to as low as 80 dB. The optimum and worst synchrophases were chosen as those giving the lowest and highest average pressure amplitude; the averages are shown at the left in the plot. The average amplitude at optimum synchrophase (0.02 psf) corresponds to 94 dB, and at worst synchrophase to a little above 103 dB.

These large variations in noise levels due to propeller phase angles indicate how large noise differences can arise between tests of the same airplane at different times. No multipropeller noise tests should be made without measuring and accounting for the effects of propeller phase angles.

Total Energy

It is obvious from the 3:1 variation of the averages that the total sound energy that gets into the fuselage is significantly affected by synchrophase selection. The total internal sound energies differed by more than 8:1 between the maximum and optimum cases shown in Fig. 17. Previous synchrophase tests were generally inconclusive on this point. It was widely believed that synchrophase affected only the distribution of the noise, whereas it can provide significant rejection of the energy emanating from the propellers. This can occur when propellers excite similar structural modes out of phase, i.e., in cancelling phases.

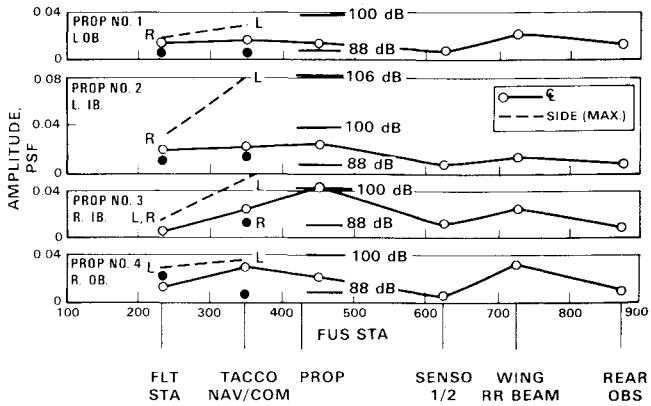

Fig. 19 68-Hz noise contributions of each propeller.

Vibration

The optimum propeller phases for minimum average vibration were found to be the same as for minimum average noise. The predicted vibration variations are shown in Fig. 18. They are generally similar to the noise data, showing that the largest variations tend to be nearest the propellers, in particular the No. 2 propeller (left inboard). For the reason that the propeller shafts are at about 2-deg angle of attack at this flight condition, the downgoing No. 2 propeller blades are highly loaded as they pass the fuselage whereas the upgoing No. 3 propeller blades are lightly loaded near the fuselage. The local blade loading affects the airborne noise transmission.

Inboard vs Outboard Propellers

The magnitudes of the 68-Hz signatures are plotted vs fuselage station in Fig. 19. Both inboards and outboards produce peaks in the cabin near the propeller plane and over the wing rear beam. In the forward cabin, the outboards are within 6-8 dB of the inboard contributions, although the airborne noise would be expected to be 12-15 dB less. The outboard propeller signatures are greater than the inboards' over the wing rear beam. These factors are evidence of the importance of the outboard propellers, and of the wing structure-borne noise, in the overall noise mechanisms in the cabin. They underline the observed importance of the outboards in setting optimum synchrophase angles.

Design Methodology

The prediction and control of interior noise and vibration of multipropeller aircraft requires consideration of propeller phase angles. This work further establishes an understanding of the vibroacoustic design problem. The advent of efficient structural and fluid dynamic finite element computer codes coupled with the practical analysis of present-day experimental acquisition equipment provides the primary factors in this assessment. The development of adaptive propeller synchrophasing equipment appears imminent and clearly offers an added dimension to the options available to the designer. The source of excitation is clear as is the advent of diagnostic methods supported by both structural and fluid dynamic methods.

Concluding Remarks

The identification and use of the noise and vibration signatures (influence vectors) of individual propellers for noise analysis and control has provided a basis for significant technological advances.

These signatures were used for 1) analytically determining optimum synchrophase angles (all 5832 combinations of 5-deg phase intervals were calculated for $4P$, $8P$, and $12P$) for minimum noise and vibration throughout the interior of the cabin, at multiples of blade passage frequency; 2) diagnosing the specific noise/vibration paths—airborne and structure-borne—that are significant in carrying the noise into the cabin.

Analysis of the signature data indicates the following.

1) Propeller synchrophasing can vary the total energy inside the fuselage volume by as much as 8:1, i.e., that synchrophasing provides significant rejection, not just redistribution, of the noise/vibration (the external energy is still there, but it does not get inside the fuselage as easily).

2) Synchrophase angles giving minimum $4P$ noise also gave minimum vibration. Low vibration is significant to equipment life as well as to habitability.

3) Outboard propellers are significant contributors to the noise and vibration in the fuselage.

4) Present synchrophasers, while useful, have typical setting errors on the order 10-15 deg and oscillate about the mean error approximately ± 5 deg in smooth air. This work indicates that synchrophasers having smaller errors are needed to achieve the potential improved habitability and equipment life extension that this research has shown to be possible. The phase-holding requirements become more necessary as the number of blades increases.

5) Optimum synchrophase angles are likely to change with equipment changes and with fuselage acoustic cavity changes. They should be determined separately for each configuration, using the propeller signature analysis techniques developed in this program.

6) Signature tests are more accurate, particularly for the higher harmonics, when they are determined from a number of different steady-state phase angles, rather than from continuously varying phase angles.

Much of the wide variability of noise measurements for a given airplane can be explained by differences in propeller phase angles; no future propeller-powered airplane vibroacoustic tests should ever be made without accurately measuring and accounting for the relative propeller phase angles.

The results and techniques from this research are directly applicable to improving the habitability and equipment life of both military and commercial propeller-powered aircraft. As such, it makes the considerable fuel-saving potential of propeller aircraft (on the order 25-30%) relative to turbofans more likely to be realized.